1-D Vortex Diffusion

Thomas S. Lund

Northwest Research Associates
CoRA Office
3380 Mitchell Lane, Boulder, CO 80301

March 16, 2015

1 Kinematics

Consider a time-dependent, 1-D, incompressible swirling flow where $u_r = 0$, $u_\theta = u_\theta(r,t)$, and $u_z = 0$. For this simple flow the vorticity reduces to a single component given by

$$\vec{\omega} = \nabla \times \vec{u} = \frac{1}{r}\frac{\partial r u_\theta}{\partial r}\hat{e}_z = \omega \hat{e}_z \tag{1}$$

The Circulation around a circular contour of radius r is

$$\Gamma(r,t) = \int_A \omega dA = 2\pi \int_0^r \omega(r,t) r dr = 2\pi \int_0^r \frac{1}{r}\frac{\partial r u_\theta}{\partial r} r dr = 2\pi r u_\theta \tag{2}$$

2 Dynamics

The mass conservation and axial momentum equations are satisfied identically. The radial and azimuthal momentum equations reduce to

$$\rho \frac{u_\theta^2}{r} = \frac{\partial p}{\partial r} \tag{3}$$

$$\frac{\partial u_\theta}{\partial t} = \frac{\partial \sigma_{r\theta}}{\partial r} + 2\frac{\sigma_{r\theta}}{r} \tag{4}$$

where $\sigma_{r\theta}$ is the viscous stress, which is given by

$$\sigma_{r\theta} = \nu_t \left(\frac{\partial u_\theta}{\partial r} - \frac{u_\theta}{r} \right) = \nu_t r \frac{\partial}{\partial r}\left(\frac{u_\theta}{r}\right) = \nu_t \left(\frac{1}{r}\frac{\partial r u_\theta}{\partial r} - 2\frac{u_\theta}{r} \right) = \nu_t \left(\omega - 2\frac{u_\theta}{r} \right) \quad (5)$$

Here we expect the flow to be turbulent and thus u_θ is the Reynolds averaged velocity and ν_t is the sum of the molecular and eddy viscosity, with the latter being a function of the radial coordinate.

By making use of the above definition of the stress it is possible to write the azimuthal momentum equation (4) in the following useful alternative form

$$\begin{aligned} \frac{\partial u_\theta}{\partial t} &= \nu_t \frac{\partial}{\partial r}\left(\frac{\sigma_{r\theta}}{\nu_t}\right) + \frac{\sigma_{r\theta}}{\nu_t}\frac{\partial \nu_t}{\partial r} + 2\frac{\sigma_{r\theta}}{r} \\ &= \nu_t \frac{\partial \omega}{\partial r} - \underbrace{2\nu_t \frac{\partial}{\partial r}\left(\frac{u_\theta}{r}\right)}_{2\sigma_{r\theta}/r} + \frac{\sigma_{r\theta}}{\nu_t}\frac{\partial \nu_t}{\partial r} + 2\frac{\sigma_{r\theta}}{r} \\ &= \nu_t \frac{\partial \omega}{\partial r} + \frac{\sigma_{r\theta}}{\nu_t}\frac{\partial \nu_t}{\partial r} \end{aligned} \quad (6)$$

An evolution equation for the vorticity can be derived from this equation by operating as follows

$$\frac{\partial \omega}{\partial t} = \frac{\partial}{\partial t}\left(\frac{1}{r}\frac{\partial r u_\theta}{\partial r}\right) = \frac{1}{r}\frac{\partial}{\partial r}\left[r\left(\nu_t \frac{\partial \omega}{\partial r} + \frac{\sigma_{r\theta}}{\nu_t}\frac{\partial \nu_t}{\partial r} \right)\right] \quad (7)$$

Equations (2) and (6) can be combined to yield the following evolution equation for the circulation

$$\frac{\partial \Gamma}{\partial t} = 2\pi r \left(\nu_t \frac{\partial \omega}{\partial r} + \frac{\sigma_{r\theta}}{\nu_t}\frac{\partial \nu_t}{\partial r} \right) \quad (8)$$

This equation can be integrated in time to give

$$\Gamma(r,t) = \Gamma(r,0) + 2\pi r \int_0^t \left(\nu_t \frac{\partial \omega}{\partial r} + \frac{\sigma_{r\theta}}{\nu_t}\frac{\partial \nu_t}{\partial r} \right) dt \quad (9)$$

Note that the integrated terms take the form of net fluxes across the circular contour at radius r. The first term is the net diffusive flux of vorticity, whereas the second is an analogous flux of the eddy viscosity. This equation demonstrates that the circulation about a fixed circular contour can only change via diffusion across the contour itself. If the contour is taken at a radius where the eddy viscosity is constant, then the circulation responds directly to the diffusion of vorticity across the contour, which is the intuitively obvious result.

Note further that Eq. (8) implies that the circulation about an infinitely large contour can not change with time. To see this, note that the vorticity is concentrated near the axis so that $\omega \to 0$ as $r \to \infty$. Thus $\partial\omega/\partial r$ must also approach 0 as $r \to \infty$. (As we will see below, the Burnham Hallock model predicts $\omega \sim 1/r^4$ and $\partial\omega/\partial r \sim 1/r^5$ as $r \to \infty$). With the vorticity concentrated near the axis, the Bio-Savart law then dictates that $u_\theta \sim 1/r$ as $r \to \infty$ and, as a consequence, $\sigma_{r\theta}/\nu_t \sim 1/r^2$ as $r \to \infty$. Physically we do not expect the eddy viscosity to grow without bound for large r and thus $\nu_t \sim r^k,\ k \leq 0$ as $r \to \infty$. Using these scaling laws, we see that $r\nu_t \partial\omega/\partial r \sim r^{k-4}$ and $(\sigma_{r\theta}/\nu_t)\partial\nu_t/\partial r \sim r^{k-2}$ as $r \to \infty$. With $k \leq 0$, both of these terms vanish for large r and we have the result $\partial\Gamma/\partial t \to 0$ as $r \to \infty$.

3 Burnham-Hallock profile

Experimentally it is observed that the vortex velocity profile is well approximated by

$$u_\theta = \frac{\Gamma_\infty}{2\pi}\left(\frac{r}{R^2+r^2}\right) \tag{10}$$

where R is the core radius and Γ_∞ is the circulation at $r \to \infty$.

3.1 Case 1: Consistent 1-D diffusion

Although the Burnham-Hallock (BH) profile contains no explicit dependence on time, it can inherit temporal variation via the parameters Γ_∞ and R (i.e. $\Gamma_\infty = \Gamma_\infty(t)$ and/or $R = R(t)$). According to the arguments made following Eq. (9), however, we expect Γ_∞ to remain fixed in time. Thus any temporal dependence in the BH model that is consistent with the 1-D flow model must come in through changes in the core radius.

In aircraft wake studies, it is found that the circulation about a fixed circular contour ($r = r_c$) decays in time at an approximately linear rate, i.e.

$$\Gamma(r_c, t) \equiv \Gamma_c(t) = \Gamma_c(0)(1 - t/\tau) \tag{11}$$

where τ is a constant that is approximately equal to $10[b_0^2/(2\pi\Gamma_c(0))]$, where b_0 is the initial separation of the vortex pair. We can use the experimentally-observed circulation decay rate to deduce the required time variation in the core radius of the BH model. First we compute the circulation from the BH model by combining Eqs. (2) and (10)

$$\Gamma_c(t) = 2\pi r_c u_\theta(r_c) = \Gamma_\infty\left(\frac{r_c^2}{R(t)^2 + r_c^2}\right) \tag{12}$$

Now combine the above two equations to get

$$\Gamma_\infty\left(\frac{r_c^2}{R(t)^2 + r_c^2}\right) = \Gamma_\infty\left(\frac{r_c^2}{R_0^2 + r_c^2}\right)(1 - t/\tau) \tag{13}$$

and then solve for R(t)

$$\frac{R(t)}{R_0} = \sqrt{1 + \left(\frac{t/\tau}{1 - t/\tau}\right)\left[1 + \left(\frac{r_c}{R_0}\right)^2\right]} \tag{14}$$

Airliners typically produce vortices with initial core radii on the order of $R_0 = 1$ meter and the circulation is typically computed on a contour of radius $r_c = 15$ meters. Thus the parameter r_c/R_0 is approximately 15. Equation (14) with $r_c/R_0 = 15$ is plotted in figure 1. This figure shows that very large changes to the core radius are required to match the observed linear circulation decay when a consistent 1-D BH model is used. The associated velocity profiles at a few select times are shown in Figure 2.

The predicted variation in the vortex core radius is in complete disagreement with experimental measurements, which show R/R_0 no larger than 2.4 out to a time of $t/\tau = 0.4$[**?**]. The consistent BH model, on the other hand, predicts $R/R_0 = 12$ at the same time. The velocity profiles shown in Figure 2 show a 80% drop in

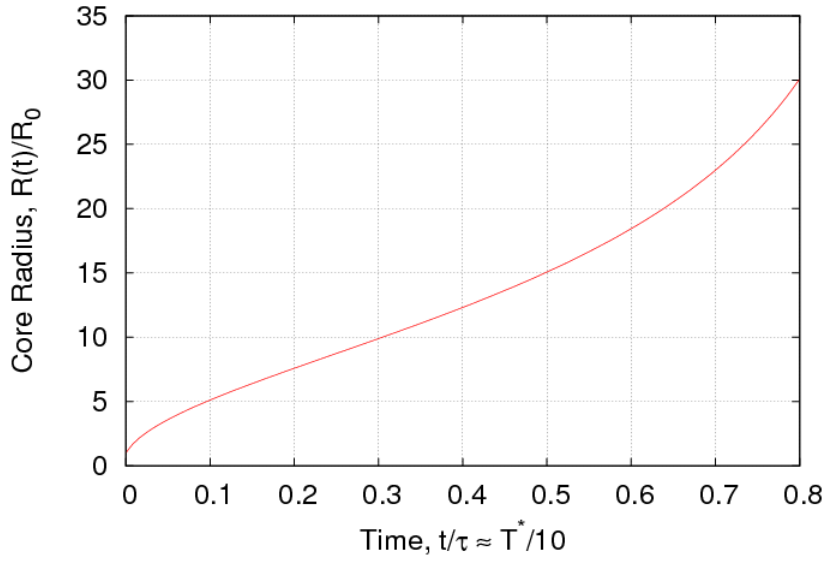

Figure 1: Temporal variation in the BH vortex core radius for a consistent 1-D model yielding a linear circulation decay rate (Eq. (14)). The parameter r_c/R_0 is set to 15.

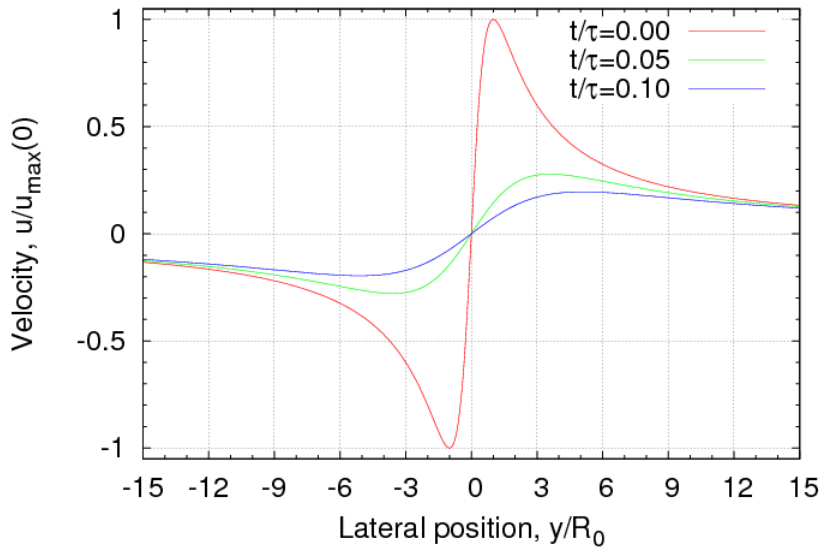

Figure 2: BH velocity profiles for a consistent 1-D model yielding a linear circulation decay rate. The parameter r_c/R_0 is set to 15. Note that $T^* \simeq 10(t/\tau)$ (i.e. $t/\tau = 0.1 \Rightarrow T^* \simeq 1.0$).

maximum velocity at a time of only $t/\tau = 0.1$ ($t* \simeq 1.0$). This feature is also in wide disagreement with experimental measurements, where the maximum velocity is observed to fall by only a few percent over a similar time interval.

The discrepancies between the model and experiments indicates that the experimentally-observed circulation decay is not associated simple 1-D diffusion with a self-similar profile having the BH shape.

3.2 Case 2: Solution with decreasing total circulation

Since the experimental data is well represented by the BH profile, independent of time, it may be possible to gain some insight by allowing Γ_∞ to vary in time. Although doing this violates conservation of circulation in the strict 1-D model, it may allow for 3-D effects that are outside its scope. If we allow $\Gamma_\infty = \Gamma_\infty(t)$, Eq. (13) can be written as

$$\Gamma_\infty(t)\left(\frac{r_c^2}{R(t)^2 + r_c^2}\right) = \Gamma_\infty(0)\left(\frac{r_c^2}{R_0^2 + r_c^2}\right)(1 - t/\tau) \tag{15}$$

According to the data presented by Delisi *et al.* (2003), the growth of the aircraft vortex core radius in time can be approximated by

$$R(t)/R_0 = 1 + 3t/\tau \tag{16}$$

The above two equations are combined and solved for $\Gamma_\infty(t)$ to yield

$$\frac{\Gamma_\infty(t)}{\Gamma_\infty(0)} = \left[\frac{1 + [(1 + 3t/\tau)^2 - 1] + (r_c/R_0)^2}{1 + (r_c/R_0)^2}\right]\left(1 - \frac{t}{\tau}\right) \tag{17}$$

This solution is plotted in Figure 3. It turns out that the term $[(1 + 3t/\tau)^2 - 1]$ which accounts for the growth in the vortex core radius is small when compared the parameter $(r_c/R_0)^2$. Thus the predicted total circulation decay is nearly the same as the observed circulation decay computed about the circle of radius r_c. This is a significant result since it seems to suggests that the observed circulation decay is largely due to some process other than simple diffusion. The term $[1 + (3t/\tau)^2 - 1]$, which accounts for diffusion of vorticity across the circle at $r = r_c$ is negligible by comparison. The velocity profiles associated with Eq. (17) are shown in Figure 4.

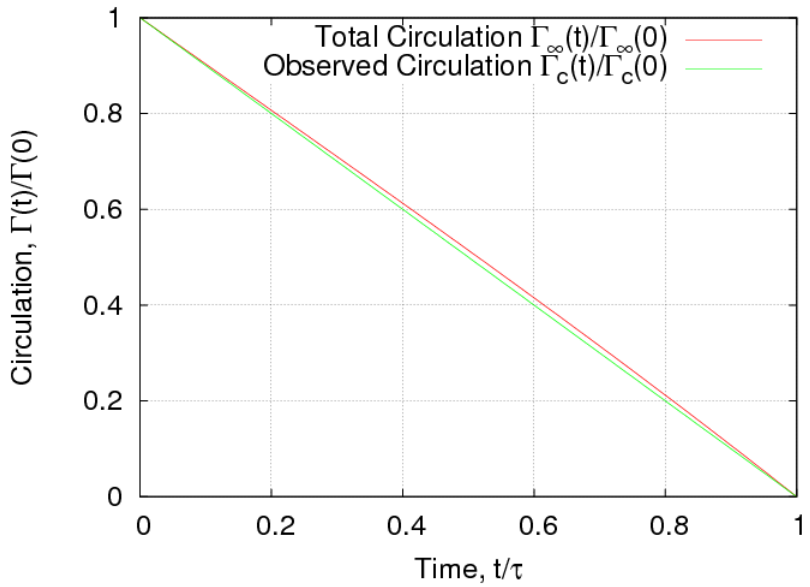

Figure 3: Temporal variation in the BH total vortex circulation required to match a linear circulation decay rate (Eq. (17), red curve). The variation in the circulation computed about the radius r_c (Eq (11)) is also shown (green curve). The model solution must be associated with 2-D effects. The parameter r_c/R_0 is set to 15.

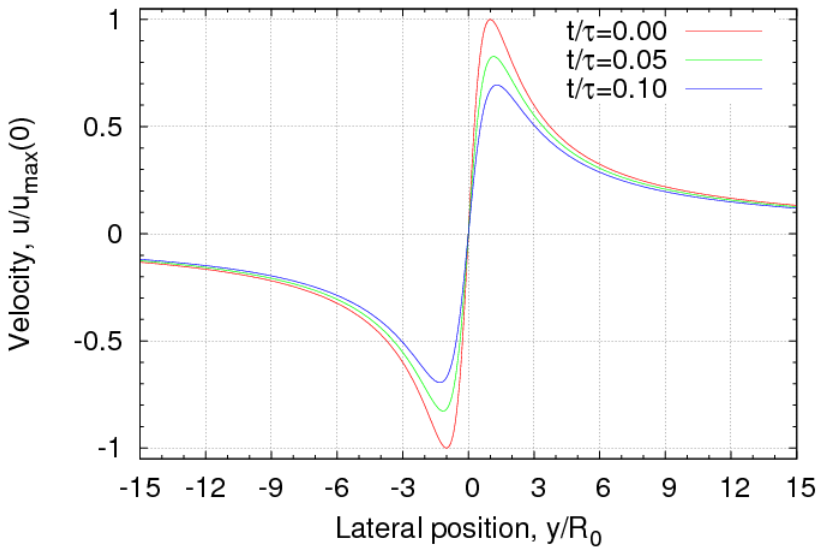

Figure 4: BH velocity profiles associated with a linear circulation decay rate for the model accounting for 2-D effects. The parameter r_c/R_0 is set to 15.

4 Mathematical model for decreasing total circulation

The experimental results of Delisi *et al.* (2003) and Burnham and Hallock (2013), as well as the analysis in the previous section all suggest that the decay of an aircraft vortex wake pair can be modeled via the BH profile with a nearly constant core radius but a time-dependent total circulation. While variable total circulation violates conservation of circulation for the strict 1-D equations governing the diffusion of an isolated vortex, it is likely that it can account for the multi-dimensional effects embodied in detrainment of vorticity as well as the annihilation of vorticity due to merger near the pair centerline. Thus it is of interest to determine whether or not it is possible to build a complete mathematical model for a BH profile with fixed core radius but decaying total circulation. Such a model is achieved by determining an eddy viscosity distribution that, when substituted into Eq. (6), yields a linear decay in the circulation measured at $r = r_c$ while preserving the BH profile shape with fixed core radius.

We start the analysis by requiring that velocity profile obey Eq. (10) with R fixed but Γ_∞ variable in time. Equations (10), (1) and (5) then give the following expressions for the velocity time derivative, the vorticity, its radial derivative, and the shear stress

$$\frac{\partial u_\theta}{\partial t} = \left(\frac{\Gamma_\infty}{2\pi}\right)\left[\frac{r}{R^2+r^2}\right]\left(\frac{1}{\Gamma_\infty}\frac{d\Gamma_\infty}{dt}\right) \tag{18}$$

$$\omega = 2\left(\frac{\Gamma_\infty}{2\pi}\right)\frac{R^2}{[R^2+r^2]^2} \tag{19}$$

$$\frac{\partial \omega}{\partial r} = -8\left(\frac{\Gamma_\infty}{2\pi}\right)\frac{rR^2}{[R^2+r^2]^3} \tag{20}$$

$$\frac{\sigma_{r\theta}}{\nu_t} = -2\left(\frac{\Gamma_\infty}{2\pi}\right)\frac{r^2}{[R^2+r^2]^2} \tag{21}$$

The circulation at radius r_c is given by Eq. (12), but with Γ_∞ variable in time and R fixed

$$\Gamma_c(t) = 2\pi r_c u_\theta(r_c) = \Gamma_\infty(t)\left(\frac{r_c^2}{R^2+r_c^2}\right) \tag{22}$$

This equation implies

$$\frac{1}{\Gamma_\infty}\frac{d\Gamma_\infty}{dt} = \frac{1}{\Gamma_c}\frac{d\Gamma_c}{dt} = -\left(\frac{1}{\tau - t}\right) \tag{23}$$

where the rightmost expression comes from Eq. (11). Now when Eqs. (18)-(21) and (23) are substituted into Eq. (6) and the result simplified, the following equation for the eddy viscosity arises

$$\frac{\partial \nu_t}{\partial r} + 4\nu_t\left[\frac{R^2}{r(R^2+r^2)}\right] - \frac{1}{2(\tau - t)}\left[\frac{R^2+r^2}{r}\right] = 0 \tag{24}$$

The solution to Eq. (24) is

$$\nu_t(r,t) = \frac{1}{4}\left(\frac{R^2}{\tau}\right)\frac{\left[1+(r/R)^2\right]^2}{(r/R)^4(1-t/\tau)}\left\{\left(\frac{r}{R}\right)^2 - \ln\left[1+\left(\frac{r}{R}\right)^2\right]\right\} \tag{25}$$

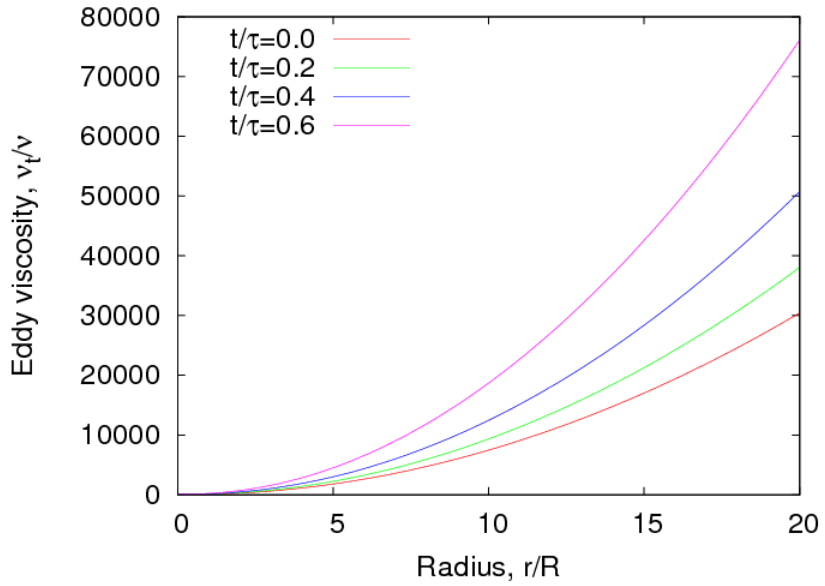

Figure 5: Eddy viscosity profiles for linear circulation decay and fixed BH velocity profile shape. The eddy viscosity is normalized by the molecular viscosity. The solutions were generated for $\Gamma_\infty = 600\ m^2/s$, $b_0 = 45.5\ m$ and standard atmospheric conditions.

The results are shown in Figure 5. Profiles are shown for various times as Eq. (25) dictates that the eddy viscosity be time-dependent. Note that the eddy viscosity is small at the origin and increases with radius. This is consistent with the picture of little or no turbulence within the core and increased turbulent transport outside of the core. Also note that the eddy viscosity is increased by the multiplicative factor $1/(\tau - t)$ as time increases. This is a somewhat curious feature of the solution that is required in order to force the linear circulation decay.

While exact, Eq. (25) is complicated in form. The following matched asymptotic approximation is quite a bit simpler and can be used to more readily asses the behavior of the solution.

$$\nu_t(r,t) \simeq \frac{1}{4}\left(\frac{R^2}{\tau}\right)\left[\frac{1/2 + \alpha(r/R)^2}{(1 - t/\tau)}\right]; \qquad \alpha = 1 \tag{26}$$

This approximation is exact in both limits $r \to 0$ and $r \to \infty$ and is a fairly good approximation in between. Its accuracy at intermediate r can be increased at the expense of some asymptotic error at $r \to \infty$ by taking the parameter α away from 1 slightly. Figure 6 shows a comparison of the exact and approximate solutions for $\alpha = 0.989$.

Although our solution for the eddy viscosity is probably reasonable out to a several multiples of the vortex core radius, it has the physically implausible divergent form $\nu_t \sim r^2$ for $r \gg R$. Returning to the discussion following Eq. (9), this is precisely the variation (i.e. $k = 2$) required in order to give $d\Gamma/dt \neq 0$ as $r \to \infty$. Thus our physically inconsistent demand that $d\Gamma_\infty/dt \neq 0$ for the 1-D equation system precipitated a physically impossible eddy viscosity distribution as $r \to \infty$. Although this aspect of the solution is unsettling, we may be able to ignore this detail if we are

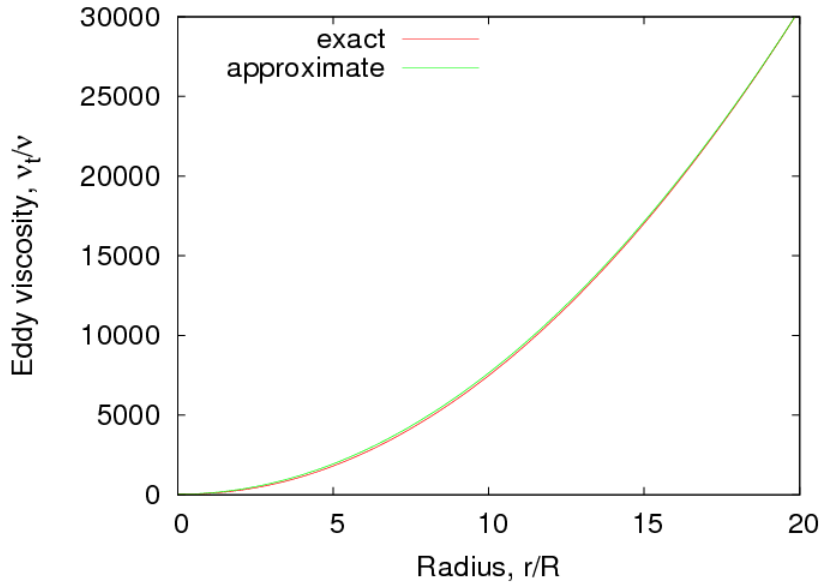

Figure 6: Comparison of the exact and approximate solutions for the eddy viscosity.

interested only in the solution out to 10-20 multiples of the core radius. After all, our intent was to see if there is a way to incorporate multi-dimensional effects in a 1-D model.

Now let us return to the solution of Eq. (6) in conjunction with the eddy viscosity distribution given by the solution to Eq. (24). The resulting circulation decay and velocity profiles are shown in Figures 7 and 8. The expected linear circulation decay is recovered and there is very little difference between the solutions with the exact or approximate eddy viscosity distribution. The velocity profiles appear to have constant BH shape with fixed core radius. The quality of the profile shape can be determined more precisely by normalizing the velocity by the instantaneous circulation. This is done for both the solutions with the exact and approximate eddy viscosity distributions in Figure 9. The results for the exact eddy viscosity distribution (Eq. (25)) are shown by solid curved on the right half of the graph and those using the approximate solution (Eq. (26)) are shown by dashed curves on the left half. While the profile shape is somewhat variable when the approximate eddy viscosity distribution is used, the collapse is perfect when the exact distribution is used. Thus the details of the profile shape are sensitive to errors in the eddy viscosity distribution whereas the circulation is largely unaffected.

As mentioned earlier, a curious feature of our solution is that the eddy viscosity is predicted to increase in time like $1/(\tau - t)$. The simple reason for this is that a constant circulation decay rate can only be accomplished in the presence of diminishing gradients via an offsetting increase in the diffusion coefficient. Although the reason for the temporal dependence is clear, it is unsettling since, if anything, one would expect the eddy viscosity to decrease in time as the gradients that sustain the turbulence decay. Thus we are motivated to investigate how the circulation decay is affected if the predicted temporal dependence is suppressed and the eddy viscosity distribution is held fixed in time. Results of such a test are shown in Figure 10. As expected, the decay is non-linear when a static eddy viscosity distribution is used.

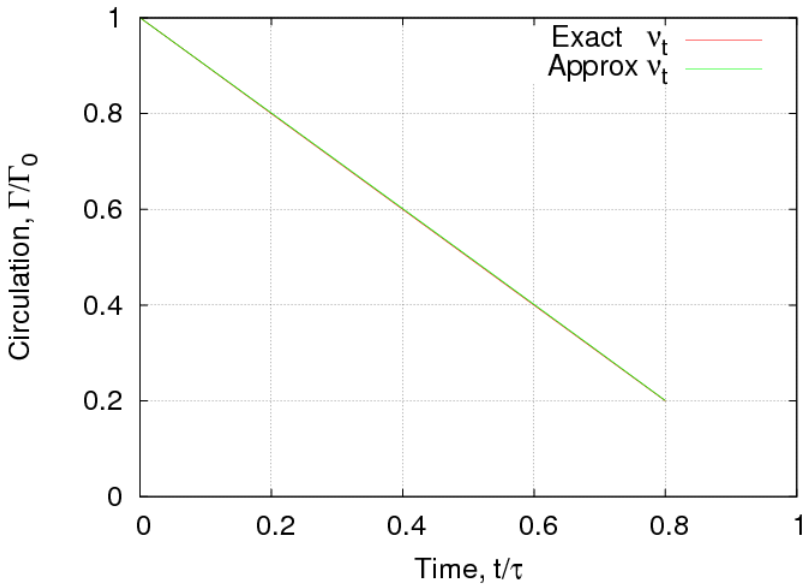

Figure 7: Computed 15 m circulation decay when Eq. (6) is solved using the eddy viscosity distribution given by Eq. (24). Results are also shown when the approximate eddy viscosity distribution given by Eq. (26) is used. The solution is for $\Gamma_\infty = 600m^2/s,\ b_0 = 45.5\ m$ and standard atmospheric conditions.

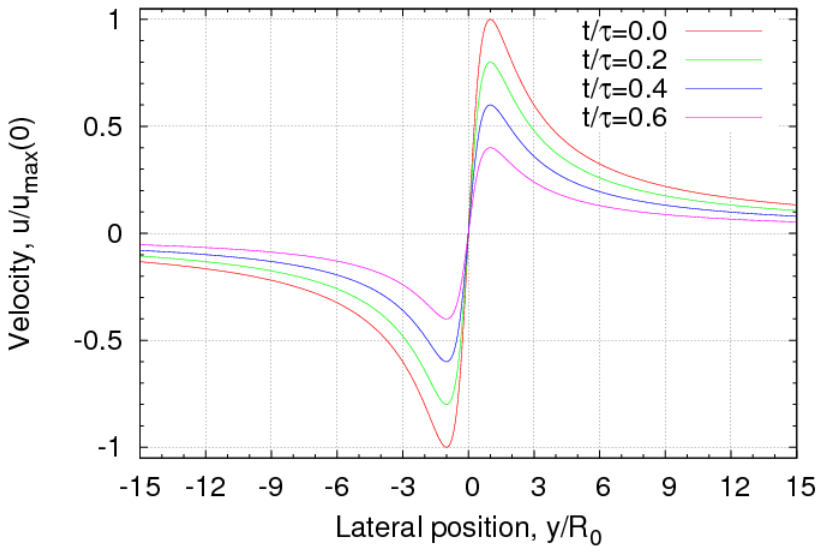

Figure 8: Velocity profiles computed from Eq. (6) using the eddy viscosity distribution given by Eq. (25). The solution is for $\Gamma_\infty = 600m^2/s,\ b_0 = 45.5\ m$ and standard atmospheric conditions.

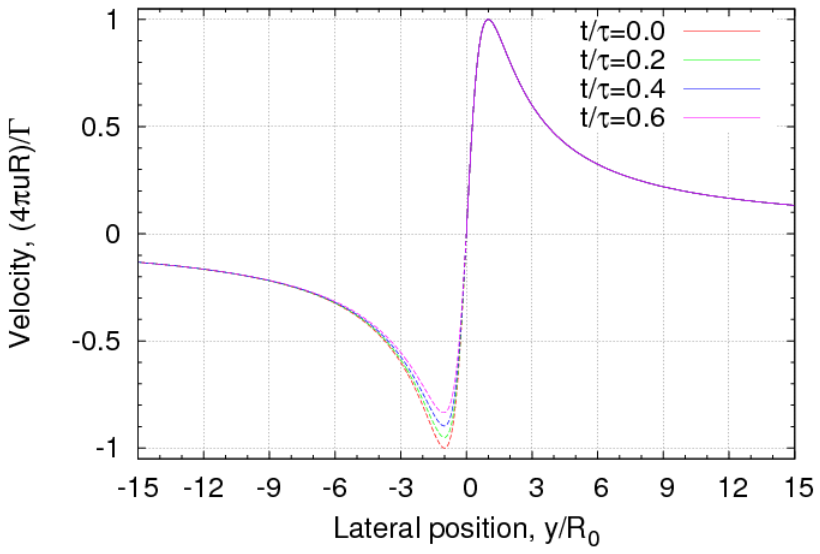

Figure 9: Scaled velocity profiles computed from Eq. (6) using the eddy viscosity distribution governed by Eq. (24). Results using the exact eddy viscosity distribution (Eq. (25)) are shown by solid curved on the right half of the graph and those using the approximate solution (Eq. (26)) are shown by dashed curves on the left half.

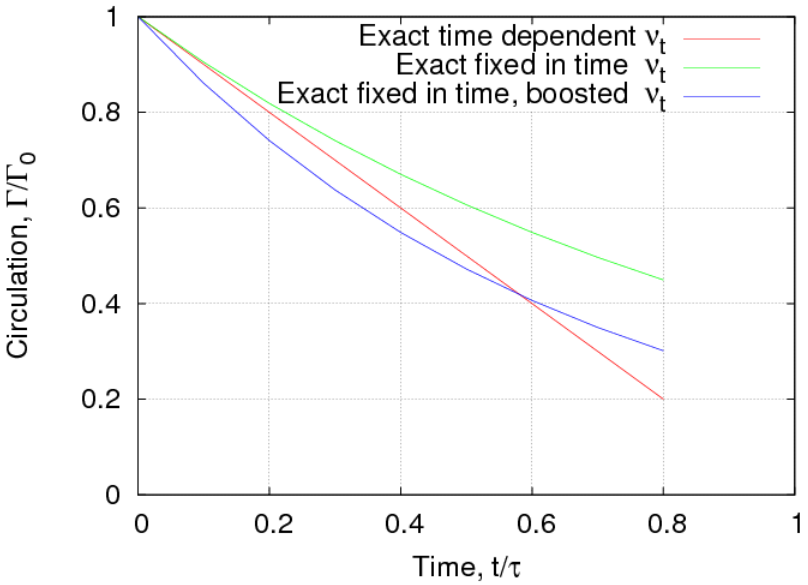

Figure 10: Computed 15 m circulation decay using both time-varying and static eddy viscosity distributions. The "boosted" curve uses a static eddy viscosity distribution that is multiplied by a constant factor of 1.5.

However, the results are reasonably close to the anticipated linear decay, especially if the eddy viscosity is boosted by a a factor designed to produce an average slope that matches the observed linear decay rate.

One might suppose that a constant circulation decay rate could be achieved with a static eddy viscosity distribution if the core radius is allowed to vary in time. This prospect was investigated but found to be a false hope since the velocity profile ceases to depend on R when $r/R \gg 1$. Thus one has no authority to control the solution via a dR/dt term when r is large.